

Contributions from Λ hyperons to nucleosynthesis in kilonovae

O. G. Benvenuto^{1,3} and E. Bauer^{2,3,*}

¹*Instituto de Astrofísica de La Plata, IALP, CCT-CONICET-UNLP, Paseo del Bosque S/N, B1900FWA La Plata, Argentina*

²*Instituto de Física de La Plata, IFLP, CCT-CONICET-UNLP, Diagonal 113 y 63 S/N, B1900 La Plata, Argentina*

³*Facultad de Ciencias Astronómicas y Geofísicas, Universidad Nacional de La Plata, Paseo del Bosque S/N, B1900 La Plata, Argentina*



(Received 5 December 2020; accepted 21 July 2021; published 4 August 2021)

We study the expansion of neutron star (NS) matter containing hyperons Λ from high densities up to the end of nucleosynthesis. This process should occur in NS-NS or NS-black hole collisions. Hyperons Λ decay by mesonic and nonmesonic reactions on a very short timescale to form proton and neutron matter. When material becomes diluted enough, the formation of helium and heavier nuclei releases energy and increases its temperature to reach nuclear statistical equilibrium (NSE) conditions with high entropy per baryon. From then on, nucleosynthesis proceeds and the final composition is largely determined by the proton per baryon fraction Y_p . We consider a recent equation of state that considers the presence of Λ hyperons [D. Logoteta, I. Vidaña, and I. Bombaci, *Eur. Phys. J. A* **55**, 207 (2019)] and simultaneously allows for the existence of NSs with masses $M \gtrsim 2M_\odot$. We assumed the composition of NS matter at densities above the threshold for the occurrence of Λ hyperons and computed its decay, finding that it appreciably increases Y_p . Then, we computed the subsequent nucleosynthesis starting from NSE assuming that the density falls exponentially. We find that, depending on the initial composition of the ejected material, the increase in Y_p due to hyperon decay is sufficient to sizeably affect the final isotopic composition of ejected matter (for example, lanthanide production may be strongly inhibited). These results indicate that Λ hyperons may affect the final composition of matter ejected in kilonova events. We also discuss the case of pure Λ matter as a possible scenario for the collision by strange stars, where we have obtained values $Y_p \approx 0.4$ – 0.5 , which leads to final isotopes far lighter than in the former case.

DOI: [10.1103/PhysRevC.104.025801](https://doi.org/10.1103/PhysRevC.104.025801)

I. INTRODUCTION

The compact stars historically named neutron stars (NSs) nowadays represent one of the most interesting objects in the cosmos. Their existence provides important information from the astronomical point of view, and also as a test laboratory for our physical models. The landmark measurement of gravitational waves (GWs) by the Laser Interferometer Gravitational Wave Observatory (LIGO) [1] has opened a new field of research in astronomy: gravitational wave astronomy. GWs can be measured from black hole–black hole (BH-BH) merges, but also from BH-NS, and NS-NS merges. Astronomers recently observed the GW source GW170817 and identified its electromagnetic counterpart, designed as AT 2017gfo, revealing a very detailed picture of these events [2].

The improvements in observational information establish a dialectic interaction between the theoretical models and data. After the discovery of the neutron by Chadwick [3], the proposal of the existence of NSs was a hypothesis due to Baade and Zwicky [4], and it took a bit more than thirty years until the first observations by Hewish and Okoye [5]. From then on, through observational information we have some

certainty about macroscopic properties of a NS like its mass, radio, angular velocity, and the intensity of the magnetic field. Because of the character of the electromagnetic signal from a NS, they received their denomination as pulsar, magnetar, etc. A summary of this classification can be found in [6].

The first models for the composition of NSs considered that these objects are made up of neutrons and protons (i.e., nonstrange hadrons). Several equations of state (EOS) were proposed, and by integrating the Tolman-Oppenheimer-Volkoff equations of hydrostatic equilibrium in general relativity a variety of NS models have been constructed; see, e.g., [7]. More recently, the structure of NSs has been studied, for example in [8], and the topic was reviewed in [9,10]. Regarding the possible presence of strange hadrons in NSs, this was proposed long ago by Ambartsumyan and Saakyan [11], and studied more recently by Glendenning [12] and by Glendenning and Moszkowski [13]. An even more extreme hypothesis is that NSs are actually quark stars with strangeness per baryon $S \approx -1$. Following the proposals of Bodmer [14] and Witten [15], this possibility was further studied by, e.g., Alcock *et al.* [16] and seriously challenged by Bethe and Brown [17] and by Alpar [18]. A third possibility is that NSs have a quark core, surrounded by hadron matter. This is usually called a hybrid star (see, e.g., [19]). The problem of the EOS of matter inside NSs is still a topic of great interest, especially since the discovery of the existence of very massive

*Corresponding author: bauer@fisica.unlp.edu.ar

objects PSR J1614–2230 with $1.928 \pm 0.017 M_{\odot}$ [20], PSR J0348+0432 with $2.01 \pm 0.04 M_{\odot}$ [21], and particularly PSR J0740+6620 with $2.14^{+0.10}_{-0.09} M_{\odot}$ [22].

An important issue is the possibility of getting some observable indication of the presence of some strangeness content inside NSs. Regarding hyperons, Sekiguchi *et al.* [23] performed numerical calculations of the NS merger process, finding that hyperons affect the dynamics and the GW radiation of the merger in a potentially detectable way. An equivalent result has been found for the case of quark matter in [24,25].

One of the most challenging problems in astrophysics is to identify the origin of chemical elements. For the case of isotopes heavier than iron, it is well known from long ago (see [26,27]), that most of their abundances are due to neutron captures. One of the processes responsible for the existence of these elements is the so called *slow* neutron capture (or simply *s* process) in which nuclei evolve on or very close to the stability valley. This mechanism, occurring during hydrostatic stellar evolution, is well understood [28] and involves isotopes which are well measured in the laboratory.

The other process is the rapid neutron capture, which is considered to be responsible for the existence of other elements like europium, osmium, platinum, etc. In this case, nuclei should be in a medium with a very large density of free neutrons. Some time ago, the *r* process was considered to take place in the core collapse of supernovae (see, e.g., [29]). However, nowadays it is considered that the most likely scenario for this process is a NS-NS or NS-BH collision. We should note that this possibility was studied long ago by Lattimer and Schramm [30]. A recent review on the *r* process was presented by Cowan *et al.* [31].

If matter that underwent *r* process captures suddenly decompresses, the very neutron rich nuclei undergo a sequence of β decays towards the stability valley, releasing enough energy to make the collision remnant shine for a while. This is what it is usually called as a kilonova. The first detection of an infrared source associated with a gamma-ray burst compatible with a kilonova event was announced in [32]. More recently, as stated above, the event GW170817 was detected by Abbott *et al.* [2] as a NS-NS merger together with the associated electromagnetic signal AT 2017gfo. These unprecedented observations provide fundamental information to investigate the characteristics of these mergers and also the nucleosynthetic results. Kasen *et al.* [33] have presented a model for the nucleosynthesis and the light curve for the AT 2017gfo event, strongly arguing that this was a kilonova. They found two components in the ejecta: one composed of light isotopes with $A < 140$ and another of heavier isotopes with $A > 140$. Simultaneously, analyzing the spectra of this event, Pian *et al.* [34], found that the data are compatible with an ejection of $2\text{--}5 \times 10^{-2} M_{\odot}$ matter containing high opacity lanthanides. Further analysis of the spectra allowed identification of the presence of strontium in the remnant [35].

In this paper we shall focus on the problem of the strange component present within a NS. We shall consider that the matter that undergoes expansion has an initial composition containing Λ particles. In particular, we shall consider a recent model presented by Logoteta *et al.* [36], where an EOS

containing Λ particles was developed. Usually, it is considered that neutron matter is softened by the presence of hyperons, making it difficult to account for the existence of the most massive NSs referred to above. Reference [36] employed a nucleon-nucleon-lambda ($NN\Lambda$) three-body force, together with realistic nucleon-nucleon, nucleon-nucleon-nucleon, and nucleon-hyperon interactions, to calculate the EOS within the many-body nonrelativistic Brueckner-Hartree-Fock approach. It is shown that the inclusion of the $NN\Lambda$ force leads to an equation of state stiff enough such that the resulting NS maximum mass is compatible with the largest currently predicted maximum mass $M_{max} \gtrsim 2M_{\odot}$.

Below, we develop a formalism which starts with hot dense matter containing Λ 's at supranuclear densities and ends with nuclei. This is done in two stages: first the Λ matter decays into protons, neutron, and pions; this system further expands and cools down. Finally, nucleosynthesis takes place. Considering the complexity of the whole kilonova event, we prefer to study the effects due to the presence of Λ 's in a very simplified way in order to gain a clear understanding of their effect on final nucleosynthetic results.

Let us discuss now the mean lifetimes of the particles involved in our model. All these times correspond to decays in free space. For the Λ -particle decay we have $\tau_{\Lambda} \approx 2.6 \times 10^{-10}$ s. The products of the Λ decay are protons, neutrons, and $\pi^{0(-)}$. Protons are stable and neutrons decay after 841 s, a time which we also consider as stable. The π^0 decays through $\pi^0 \rightarrow 2\gamma$ with a branching ratio (BR) of 0.98823. From this, the π^0 has no effect in our calculation. The π^- decays mainly as $\pi^- \rightarrow \mu^- + \bar{\nu}_{\mu}$, with a BR = 0.999 877 and $\tau_{\pi^-} \approx 2.6 \times 10^{-8}$ s. The μ^- can interact with the proton, leading to a change in the relative population of protons and neutrons. These reactions are $\mu^- + p \rightarrow \nu_{\mu} + n$ and $\mu^- + p \rightarrow \nu_{\mu} + n + \gamma$. The importance of these reactions depends on our model for the expansion of the whole system. In any case, at this stage we neglect any reaction but Λ decay itself. The values of all decay widths and BR were taken from [37].

In summary, in this work we evaluate the partial contribution to the nucleosynthesis of elements from hot, dense matter containing Λ 's ejected from a NS-NS merger. We model this process by evaluating microscopically the Λ decay and considering that no further decays or reactions take place until nucleosynthesis operates. We consider also the extreme case of pure Λ matter, which is a theoretical possibility in the collision of strange stars. Our results should be interpreted as a partial contribution to the whole problem of kilonovae.

This work is organized as follows. In Sec. II, we discuss the different Λ decay mechanisms in a dense medium and briefly describe the techniques we employed to compute the final nucleosynthesis. Our results are discussed in Sec. III, where we give special attention to the initial Λ decay and the nucleation conditions. Finally, in Sec. IV we discuss the relevance of our results and give some conclusions.

II. FROM DENSE MATTER WITH Λ HYPERONS TO NUCLEI

As mentioned in Sec. I, our concern in this work is the final isotopic composition resulting from matter ejected in a

kilonova event. More specifically, we consider matter composed of protons, neutrons, and Λ particles. The Λ particle is the lightest hadron with strangeness and its properties are better understood than other strange particles. Due to this, it is the natural choice as the starting point for nucleosynthesis from the strange component of NSs. One should keep in mind that within a NS it is the gravitational force that is responsible for the high densities of the system. Ejected matter will expand due to the weakening of the gravitational attraction. In this fast decrease of density which starts with hot dense matter containing Λ particles and ends with nuclei, we define two stages:

- (i) In the first stage, we start with matter which contains different proportions of Λ particles, until their exhaustion. We assume values for the initial density, entropy per baryon, s , and a model for the expansion of the system. The final products of this decay process are neutrons, protons, and pions. From the decay process, we obtain the final fraction of protons per baryon, Y_p , together with the final temperature and density.
- (ii) The second stage is the time interval from Λ particles exhaustion up to the end of the nucleosynthesis.

In the next subsections we address these points in detail.

A. The Λ hyperon decays

Let us consider hot matter with a partial or total content of Λ particles, at high density. The Λ particle has several decay modes induced by the weak interaction. In free space, the Λ decays via the so-called mesonic decays, namely,

$$\Lambda \rightarrow n\pi^0, \quad (1)$$

$$\Lambda \rightarrow p\pi^-. \quad (2)$$

In a nuclear medium we have to add the nonmesonic decays,

$$\Lambda n \rightarrow nn, \quad (3)$$

$$\Lambda p \rightarrow np. \quad (4)$$

For each of them we define the corresponding decay widths as

$$\begin{aligned} \Gamma_{\pi^0} &\equiv \Gamma(\Lambda \rightarrow n\pi^0), \\ \Gamma_{\pi^-} &\equiv \Gamma(\Lambda \rightarrow p\pi^-), \\ \Gamma_n &\equiv \Gamma(\Lambda n \rightarrow nn), \\ \Gamma_p &\equiv \Gamma(\Lambda p \rightarrow np). \end{aligned} \quad (5)$$

These decay widths depend on the partial densities of each kind of particle and on the temperature of the system. In Figs. 1 and 2, we show the Feynman diagrams for the transition amplitude for each decay width. By inspection of these transition amplitudes, we should emphasize that the only source of protons is reaction (2) (associated with the Γ_{π^-} -decay width). The amount of protons in the initial and final state is the same for the reaction $\Lambda p \rightarrow np$. Note, from Fig. 2, that two transition amplitudes contribute to Γ_p : the second diagram in this figure is the direct one, while the third one is the charge exchange contribution. Note also that, Λ being a

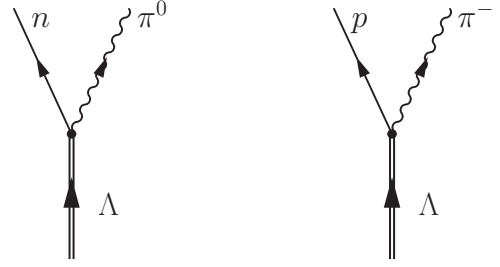


FIG. 1. Transition amplitudes for the mesonic decays Γ_{π^0} and Γ_{π^-} , respectively.

noncharged particle, charge conservation does not allow any other decay at first order in the weak interaction.

At zero temperature, explicit expressions for Γ_{π^0} and Γ_{π^-} are found in [38], while we refer the reader to [39] for the expressions for Γ_n and Γ_p . For the benefit of the reader, we give the finite temperature expressions in the Appendix, which are easily obtained from these ones at $T = 0$.

The mesonic and nonmesonic decays play different roles in the evolution of the system from matter which contains Λ particles to hadronic matter without Λ 's. To make our point clearer, let us consider pure Λ matter. In the initial time, the absence of protons and neutrons makes the mesonic decays the only possible reactions. Shortly after this, the presence of these hadrons triggers the nonmesonic decay. As the density of protons and neutrons grow, the Pauli principle inhibits the mesonic decay. There is a certain competition among the mesonic and the nonmesonic channels: while the mesonic channel favors the production of protons, the nonmesonic one gives only neutrons. The mesonic channel dominates for low densities or high temperatures, while the nonmesonic contribution is more important for high densities at low temperatures.

Before we go further, it is worth mentioning that there are others decays channels which we are not considering here. In first place we should mention the reaction $\Lambda\Lambda \rightarrow \Lambda n$. It is a nonmesonic reaction induced by the Λ particle itself and it has the peculiarity that it is active all over the decay of the Λ matter. This reaction has been studied in [40], from which we know that it gives a small contribution. Still, there are higher order nonmesonic contributions such as $\Lambda np \rightarrow nnp$

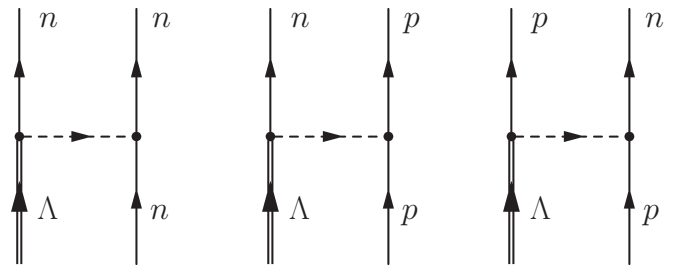


FIG. 2. Transition amplitudes for the nonmesonic decays Γ_n (first diagram) and Γ_p (second and third diagram). By a dashed line we represent the weak interaction, given by the exchange of the π , ρ , K^* , η , ω , and K mesons.

[41,42]. These reactions originate from ground state correlations and we have preferred not to include them in this work. This is because, being higher order contributions, we do not expect them to change significantly the final result.

Let us now discuss a model for the time evolution of our system, from hot matter with Λ hyperons to proton-neutron matter. Our aim is to know the proton fraction $Y_p \equiv N_p/(N_p + N_n + N_\Lambda)$, where N_i is the total number of particles of the kind i . The quantity Y_p is in fact a time-dependent function and, after all Λ particles have decayed, it is taken as an initial condition for the subsequent evolution of the system, when nucleosynthesis occurs. The link between the decay widths and the number of particles is given by the general relationship,

$$\frac{dN_f(t)}{dt} = \sum_{\alpha} \Gamma_{\alpha}(N_1, N_2, \dots, T) \prod_{i=1} N_i(t). \quad (6)$$

The index α runs over the values $\alpha = \pi^0, \pi^-, n$, and p [see Eqs. (5)], and contains in its final state the particle of kind f . The notation $\prod_i N_i(t)$ represents the product of the number of particles in the initial state: for instance, for the decay $\Gamma(\Lambda p \rightarrow np)$, $\prod_i N_i(t) = N_\Lambda N_p$. This expression results in a set of coupled first-order differential equations, where $f = \Lambda, n$, and p , together with the constrain $N = N_n(t) + N_p(t) + N_\Lambda(t) = \text{const}$. The initial conditions will be given soon.

Rather than working with the total number of particles, N_j , it is convenient to show these equations using the relative fraction of particles, defined as $\mathcal{Y}_i \equiv N_i/N$. Note also that $\mathcal{Y}_i = \rho_i(t)/\rho(t)$, where $\rho_i(t) = N_i(t)/V(t)$ is the number density, where the volume $V(t)$ depends on time. The set of Eqs. (6) are rewritten as

$$\begin{aligned} \frac{d\mathcal{Y}_n(t)}{dt} &= \Gamma_{\pi^0} \mathcal{Y}_\Lambda(t) + \Gamma_n \mathcal{Y}_n(t) \mathcal{Y}_\Lambda(t) + \Gamma_p \mathcal{Y}_p(t) \mathcal{Y}_\Lambda(t), \\ \frac{d\mathcal{Y}_p(t)}{dt} &= \Gamma_{\pi^-} \mathcal{Y}_\Lambda(t), \end{aligned} \quad (7)$$

which can finally be expressed as¹

$$\begin{aligned} \frac{d\rho_n}{dt} \rho &= \Gamma_{\pi^0} \rho_\Lambda \rho + \Gamma_n \rho_n \rho_\Lambda + \Gamma_p \rho_p \rho_\Lambda + \rho_n \frac{d\rho}{dt}, \\ \frac{d\rho_p}{dt} \rho &= \Gamma_{\pi^-} \rho_\Lambda \rho + \rho_p \frac{d\rho}{dt}, \end{aligned} \quad (8)$$

where for simplicity the explicit functional dependences of the densities and decay widths have been omitted for brevity of the notation. Notice that the last terms in the right-hand sides of these equations (i.e., $\rho_i d\rho/dt$) are always negative for an expansion. Keeping in mind that $\rho = \rho_\Lambda + \rho_n + \rho_p$, we write for completeness

$$\frac{d\rho_\Lambda}{dt} = \frac{d\rho}{dt} - \frac{d\rho_n}{dt} - \frac{d\rho_p}{dt}. \quad (9)$$

To solve this set of equations one has to specify the initial total densities $\rho_i(t=0)$, $i = n, p, \Lambda$, and the initial temperature, together with a model for the temporal evolution of density and temperature. This is discussed below, in Sec. III. The

dynamics of the decays (contained in the decay widths Γ_i), gives us the relative number of protons and neutrons or Y_p . We are aware that the inverse reactions which produce Λ particles are possible. This would affect the total time to the Λ matter decay, but it is not expected an important change in the final result for Y_p . This point is further discussed in the next section.

Before going on, we should discuss briefly the physics of the Λ decay. What we know about the Λ decay comes from two different physical sources: first, the Λ -free decay, which is well understood; second, the Λ -hypernuclei decay. We explain now why we are dealing with a third kind of problem. The Λ -free decay is dominated by the Γ_{π^0} and Γ_{π^-} , decays. These decays are induced by the weak interaction and the Λ particle has also an electromagnetic decay, whose branching ratio is negligible.

The experimental information about the Λ -hypernuclei decay comes from the emission spectra of the particles emitted in the decay; see for instance [43,44]. In these spectra one plots $N_n(E)$ and $N_p(E)$, where E is the energy of the emitted neutron and proton, respectively. Obviously $\int N_i(E) dE = N_i$. And in fact data for the N_n/N_p ratio are given. But this ratio has a different meaning than ours. This is important, because the N_n/N_p hypernuclear result must not be used in our problem. The main differences with our problem are

- (i) The spectra from the hypernuclear decay result from the decay of a large set of hypernuclei all at the same quantum state. On the other hand, in our problem, once a Λ decays, this process affects the composition (or partial density), and the next decay is different due to this change in the density.
- (ii) In the hypernuclear spectrum, $\Gamma(\Lambda p \rightarrow np)$ is a source of protons: from the Λ decay a bound proton acquires enough energy to be ejected to the continuum. The residual nucleus has one proton less and, as mentioned, in hypernuclei the $\Lambda p \rightarrow np$ decay contributes to the proton spectra. The situation for our problem is different, because the only source of protons is the Γ_{π^-} decay. Our concern is the total number of protons in the whole system and the $\Lambda p \rightarrow np$ decay does not change this number.

Briefly, the physical situation of having a set of hypernuclei, all at the same quantum state, which emit particles and leaves a residual nucleus, is different than the one of matter containing Λ particles. From this, we can assert that Λ decay discussed in this work represents a novel process.

B. The nucleosynthesis process

As matter expands, its density and temperature go down to values in which the formation of nuclei becomes possible. Then, the material undergoes the nucleosynthesis process.

In order to obtain the final isotopic abundances of the expanding matter, it is necessary to consider a large network of nuclear reactions. To tackle this problem, we have employed the TORCH code [45]. Among other capabilities, TORCH can compute the nucleosynthesis during the expansion of matter starting from nuclear statistical equilibrium conditions. All the calculations to be presented below were performed assuming

¹Note that $\frac{d\mathcal{Y}_i}{dt} = \left(\frac{d\rho_i}{dt} \rho - \rho_i \frac{d\rho}{dt}\right) \rho^{-2}$.

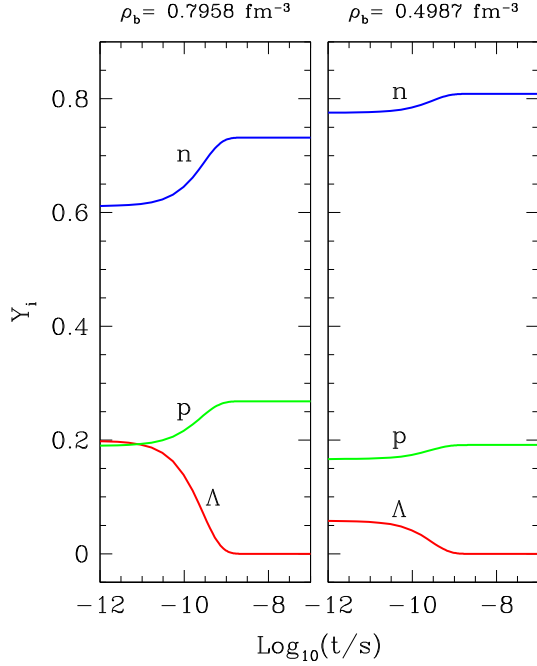


FIG. 3. Time-evolution of the Λ , neutron, and proton fractions from Eq. (7). We have shown the results for two different values of the initial baryon density, while the entropy per baryon is $3k_B$. Time is given in seconds.

a network of 3298 isotopes. Recently, Kasen *et al.* [46] have employed this code to compute nucleosynthesis in kilonovae models.

III. RESULTS

In this section we discuss our results in three subsections. First, we consider the decay of matter containing Λ particles into protons, neutrons, and pions. In a second subsection we analyze the expansion and cooling process up to the nucleosynthesis. Finally, in the third subsection we discuss the extreme case where the initial composition is entirely made out of Λ 's.

A. From Λ matter to protons and neutrons

In this initial stage, the evolution of the system is modeled with the function $\tilde{\rho}_b(t) = \rho_b e^{-t/\tau_{exp}}$, where $\tilde{\rho}_b(t)$ is the total baryonic density and the constants ρ_b and τ_{exp} will be specified soon. We consider different values for the entropy per baryon, s . We employ the equilibrium values for the partial hadronic densities from the EOS developed in [36] at zero temperature. We refer the reader to Fig. 3 (left panel) of that work to see the partial hadronic densities at equilibrium. For the benefit of the reader, we show some values for the different partial baryonic densities in Table I. We also show the proton fraction Y_p , which has been defined in Sec. II A. Within our scheme, the proton fraction depends on time and we have employed the notation $(Y_p)_{NS}$ for its equilibrium value in the NS. Note also that there is a threshold density from which we begin to have Λ particles. In this work, we also study the hypothetical pure Λ matter at twice the nuclear

TABLE I. Different initial composition of NS matter at thermodynamical equilibrium taken from [36]. Densities are given in units of fm^{-3} . For convenience we show the proton fraction $(Y_p)_{NS}$.

ρ_b	ρ_n	ρ_p	ρ_Λ	$(Y_p)_{NS}$
0.1089	0.1046	0.0042	0.0000	0.0386
0.2017	0.1873	0.0143	0.0000	0.0711
0.3038	0.2696	0.0342	0.0000	0.1127
0.4059	0.3439	0.0613	0.0007	0.1511
0.5080	0.3901	0.0851	0.0328	0.1675
0.6008	0.4220	0.1048	0.0741	0.1744
0.7029	0.4564	0.1277	0.1188	0.1817
0.8051	0.4920	0.1530	0.1600	0.1901
0.9072	0.5288	0.1808	0.1975	0.1993
1.0000	0.5627	0.2081	0.2292	0.2081

saturation density, having the initial condition $\rho_b = \rho_\Lambda = 2\rho_0$ ($\rho_n = \rho_p = 0$). For the nuclear matter saturation density, we have employed $\rho_0 = 0.16 \text{ fm}^{-3}$. Results from pure Λ matter are discussed in Sec. III C.

As mentioned, we ascribe to the expelled matter a nonzero value for the entropy per baryon. Under this assumption, matter evolves to a new equilibrium, which should be achieved through a set of reactions among the particles. In this work, we focus on the Λ decay which, as we shall show, is faster than the expansion. To reach complete equilibrium, all possible reactions have to be taken into account. In Sec. I, we called attention to a set of reactions in free space which can be relevant in this problem, where some mean lifetimes are rather slow compared to our expansion model. In this case, the model for the expansion would be as important as the reactions themselves. Our concern is the effect of the Λ decay on the final composition, assuming that the sudden change from matter at zero temperature to hot expanding matter triggers this decay. It is worth mentioning that a rather different approach would be to construct an EOS. This approximation assumes that the characteristic timescale of all possible reactions is much shorter than that of expansion and, as a consequence, matter has sufficient time to reach equilibrium. At the end of this subsection we discuss further this point by making a brief comparison between these two approaches.

We start with four different initial conditions summarized in Table II. For different initial baryonic densities ρ_b , each case has a different proportion of Λ matter; this proportion rises for increasing values of the density. For the expansion, we have taken the value $\tau_{exp} = 10^{-3} \text{ s}$, while for the entropy per baryon we consider values which range from $s = 1.0k_B$

TABLE II. Four initial composition of NS matter analyzed in this work, taken from [36]. Densities are given in units of fm^{-3} .

Case	ρ_b	ρ_n	ρ_p	ρ_Λ	$(Y_p)_{NS}$
A	0.4987	0.3867	0.0831	0.0289	0.1667
B	0.6008	0.4220	0.1048	0.0741	0.1744
C	0.7029	0.4564	0.1277	0.1188	0.1817
D	0.7958	0.4888	0.1506	0.1564	0.1893

up to $4.0k_B$. As will be clear soon, the choice of τ_{exp} is not important for this initial stage, since the Λ matter evolves on a timescale far shorter than the expansion. The weak transition potential required for the Λ decay is described in terms of the usual one-meson-exchange (OME) potential, which is represented by the exchange of π , η , K , ρ , ω , and K^* mesons within the formulation of [47], with values of the coupling constants and cutoff parameters taken from [48,49].

We go straight to the solution of the set of Eqs. (7). These equations are solved numerically and the functions $\mathcal{Y}_\Lambda(t)$, $\mathcal{Y}_n(t)$, and $\mathcal{Y}_p(t)$ are plotted in Fig. 3, where the initial conditions are the ones for Cases A and D, in Table II. In this figure we show the evolution of these fractions from the initial supranuclear density up to the decay of all Λ 's. Having in mind our expansion law, the total density remains almost constant during the Λ decay process, a point which is further discussed in this subsection.

From this figure we can evaluate the average Λ half-life—starting at $t_0 = 0$ s, the time when half of the Λ 's have decayed is $t_f \approx 10^{-10}$ s—and from this we can estimate the half-life as $\Delta t \approx 10^{-10}$ s. We recall that the Λ mean lifetime in free space is $\tau_\Lambda \approx 2.6 \times 10^{-10}$ s. The half-life is always smaller than the mean life, but still it is clear that the decay of this dense medium is faster than the free decay. We address this point because at first glance it looks contradictory: for a particular decay mechanism, in a dense medium the available phase space of final states is always smaller than in free space. But in a dense medium we also have the nonmesonic decay, which is not present in free space and ultimately enlarges the phase space. This half-life becomes smaller as the temperature grows. For increasing values of the temperature the phase space of final states is bigger, which leads to also bigger values of the decay widths (we recall that $\tau = \hbar/\Gamma$).

Going on with the analysis of Fig. 3, we consider now the different decay mechanisms as shown in Eqs. (5). The distinction between mesonic (Γ_{π^0} and Γ_{π^-}) and nonmesonic (Γ_n and Γ_p) is important due to energy considerations. To make this point clear, let us consider a Λ particle at rest. The Λ decay vertex contains the Λ particle ($m_\Lambda = 1116$ MeV), a nucleon ($m_N = 939$ MeV), and a meson. If the meson is a pion ($m_\pi = 139$ MeV), from the decay we have, $Q = m_\Lambda - m_N - m_\pi = 38$ MeV. At zero temperature and assuming that all this energy becomes kinetic energy for the nucleon, if the Fermi energy is bigger than Q , then the mesonic decay is forbidden. Equivalently, we can say that the mesonic decay is Pauli blocked. For Λ particles with kinetic energy and for finite temperature, the Pauli blocking is less effective, but it is still present.

By inspection of the Q value we notice that the pion is the only meson which can be produced in the mesonic decay. The situation is different for the nonmesonic decay. In this case, mesons are off the mass shell and we should consider all possible mesons. As we do not have any meson in the final state, the final nucleons now share an energy $\tilde{Q} = m_\Lambda - m_N = 177$ MeV, which makes it unlikely for them to be Pauli blocked. The nonmesonic decay is induced by a nucleon. This means that, in the particular case of pure Λ matter (see Sec. III C), at $t = 0$ the only possible decays are Γ_{π^0} and Γ_{π^-} . Shortly after this, there are protons and neutrons in the medium and the

decays Γ_n and Γ_p turn on. Under the initial conditions from Table II, both mesonic and nonmesonic decays are present all over the Λ decay process.

As we have already mentioned, further reactions which produce Λ particles are possible and we are not considering them. This is because no change in the lower limit of the proton fraction is expected due to these reactions. The Λ creations induced by π mesons are possible (for instance, the strong induced reaction $\pi^- + p \rightarrow K^0 + \Lambda$), but due to the difference in the rest mass of the incoming and outgoing particles these reactions are unlikely, meaning that their effect should be small in our final results. The mesonic inverse reaction, $N + n \rightarrow \Lambda + N$, with $N = n, p$, turns a neutron into a Λ particle. Afterwards, the Λ particle can decay through any of the decay channels shown in Eqs. (1)–(4). This means that some of them would add protons to the system. From these considerations, it is reasonable to assume that our values for the proton fraction are a lower limit for that quantity. We should recall that there is a threshold density for the stability of the Λ particles. For densities $\rho_b \lesssim 2\rho_0$, all Λ 's decay.

Also from Fig. 3, due to isospin considerations the Γ_{π^-} decay width is always bigger than the Γ_{π^0} one. No matter the initial composition, the mesonic decay increases the amount of protons and neutrons, reducing the phase space for the mesonic decay itself. This means that in the Λ decay process the nonmesonic decay becomes more important at the final stages of the decay. The nonmesonic decay only supplies neutrons. From both panels the general conclusion is that the decay of Λ particles increases the proton fraction.

Now we give explicit numerical values for the fraction of protons once all Λ particles have decayed. For this stage, when we have protons and neutrons, we name the proton fraction as $(Y_p)_{PN}$. We show $(Y_p)_{PN}$ as a function of the entropy per baryon (or equivalently as a function of the temperature) in Table III. From this table we notice that as the entropy per baryon grows, so does $(Y_p)_{PN}$. This is because the mesonic decay becomes more important when the temperature rises. In any case, this value saturates at $(Y_p)_{PN, max} = 2/3$, which is the value where the nonmesonic decay plays no role. The values of $(Y_p)_{PN}$ are the main result of this subsection; they are employed as inputs for the next step. Finally, the Λ decay process is very fast and the initial conditions of temperature and density are almost unchanged during the Λ decay. For consistency, we have considered these changes, but due to their magnitude it is not worth tabulating them.

As mentioned, the Λ decay process is very fast relative to the expansion. To show this point, we have also solved the set of Eqs. (8), under the same conditions of Fig. 3. These results are depicted in Fig. 4. We show the evolution of the functions $\rho_\Lambda(t)$, $\rho_n(t)$, and $\rho_p(t)$ from the initial supranuclear density up to a density slightly below ρ_0 . In this figure, due to our expansion law, it is clearer that the total density remains almost constant during the Λ decay process, as we have already discussed. Having in mind that time is plotted in a logarithmic scale, the drop in $\rho_n(t)$ and $\rho_p(t)$ at $t \approx 10^{-4}$ s is due to the expansion. In the same figure we have superimposed the dimensionless proton fraction Y_p as a function of time, which shows that this fraction remains constant after all Λ 's have decayed.

TABLE III. Proton fraction when all Λ particles have already decayed. We show the conditions at which NS matter undergoes hyperon decay. From left to right we list the initial condition considered (given in Table II), the considered entropy per baryon (in units of the Boltzmann constant), the temperature (given in MeV) at which the process occurs, and the final value of the proton per baryon abundance, $(Y_p)_{PN}$. Due to the timescale of the Λ decay, the final baryonic densities are approximately the same as the ones in Table II).

Case	s	T	$(Y_p)_{PN}$
A	1.0	7.1189	0.1803
B	1.0	8.0053	0.2038
C	1.0	8.8373	0.2209
D	1.0	9.5118	0.2324
A	2.0	14.861	0.1873
B	2.0	16.711	0.2183
C	2.0	18.448	0.2408
D	2.0	19.856	0.2570
A	3.0	23.594	0.1913
B	3.0	26.483	0.2262
C	3.0	29.189	0.2507
D	3.0	31.381	0.2681
A	4.0	34.040	0.1942
B	4.0	38.136	0.2314
C	4.0	41.967	0.2569
D	4.0	45.065	0.2748
A	5.0	46.725	0.1963
B	5.0	52.250	0.2351
C	5.0	57.409	0.2611
D	5.0	61.575	0.2792
A	6.0	60.949	0.1979
B	6.0	67.903	0.2376
C	6.0	74.375	0.2640
D	6.0	79.585	0.2821

Before we end this subsection, we turn back to the alternative approach of considering the results from an EOS model. In Fig. 2 in [50], the authors depicted the relative particle fractions as functions of baryon density in beta-equilibrated matter using different entropies, starting from zero. We are interested in the low density region, where there is no Λ 's. We notice an increase of the proton fraction for increasing values of the entropy per baryon. This result is in qualitative agreement with ours, where our proton fraction has increased for the same conditions. Beyond this qualitative agreement, the physical origin of this result is different. Our increase in the proton fraction is due to the Λ decay, while the EOS has no memory of the former configurations. As we have stated, this depends on the timescale of the reactions involved compared with the expansion times. There is no contradiction between the approaches: if the time is long enough, all possible reactions take place and eventually the reactions would erase the information about the Λ component of matter. On the other hand, if the expansion does not allow all the needed reactions for equilibrium, then the EOS result is not accurate for this problem. In any case, our scheme and the EOS approach

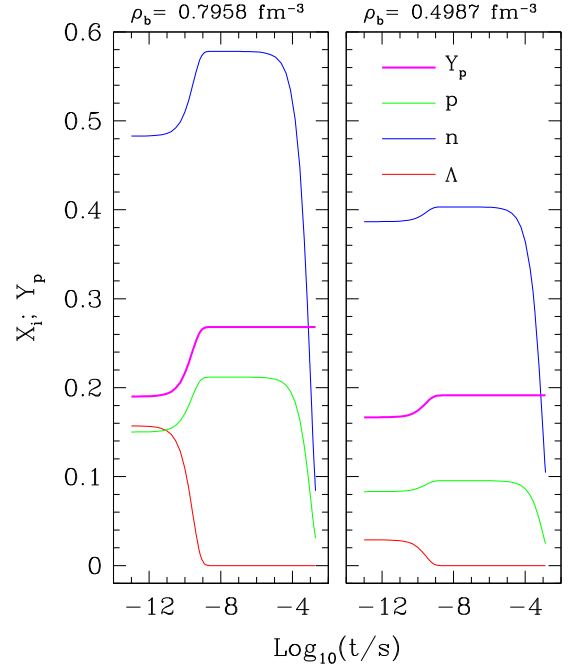


FIG. 4. The same as Fig. 3, but for the time evolution of the Λ , neutron, and proton densities from Eq. (8).

can be thought of as two extreme models. The fact that both predictions are in agreement suggests that the actual physical situation is close to both models.

The evolution of matter, from the equilibrium conditions in the NS to low densities, requires a time-dependent model which must consider both the expansion and the reactions needed to restore equilibrium. We have shown that the microscopic description for the Λ decay is important and the method to evaluate this decay is particular to this problem. We have also shown that the Λ decay is very fast, which means that, no matter how rapid the expansion is, all Λ 's will decay. Once all Λ 's have decay, we freeze the composition.

B. Nucleosynthesis

Here we shall present our results on the nucleosynthesis of NS matter after its decompression. Freiburghaus *et al.* [51] have shown that the conditions of temperature and density at which nucleosynthesis occurs are largely independent of the values at which matter is ejected. Indeed, the formation of helium and heavier nuclei results in an energy release so large that it increases the temperature of the matter to reach conditions of NSE. Because of this reason, following [46], for this final stage of evolution we shall assume that matter initially is in NSE and with a temperature of 5×10^9 K undergoing expansion with a constant value for entropy per baryon of $s = 20k_B$, and density falling down exponentially with a timescale of $\tau_{exp} = 0.1$ s. The conditions from which we start out these calculations are based on the results presented by Fernández and Metzger [52] related to the dynamics of outflows after NS coalescence, in particular their Fig. 5. At conditions of higher densities and temperatures the material stays in NSE since nuclear reactions are faster than

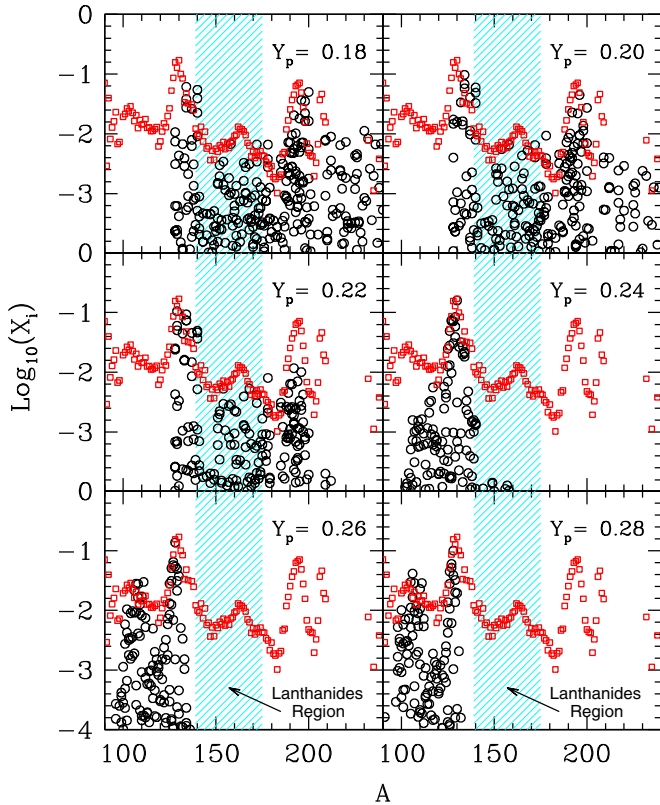


FIG. 5. Nucleosynthesis resulting from the expansion of matter for different values of the proton per baryon abundance, $(Y_p)_{PN}$, covering the range of values found by expanding the hyperon rich matter (see Table III). Red squares represent the abundances due to the r process given in [53], shifted $10^{(7.5)}$ upwards for graphical purposes. Abundances are given in mass fractions.

decompression. However, this is no longer valid for temperatures lower than 5×10^9 K. So, in these conditions it is unavoidably necessary to perform a detailed nucleosynthetic calculation. TORCH does not include a treatment of fission; so, we followed the calculations up to the moment in which temperature falls to 10^6 K. This represents a timescale of only 2.58 seconds. Notice that among the final abundances to be presented below, many of them correspond to unstable nuclei. As stated above, the aim of this paper is to study the effects of the presence of Λ hyperons in the final nucleosynthesis of a kilonova event. So, we consider that the treatment presented in this paper is detailed enough to show that hyperons have a non-negligible effect on the final abundances of these events. In order to perform a more detailed treatment of the whole kilonova event we would need, among other things, to include fission in this treatment. This is beyond the scope of this paper.

The resulting nucleosynthesis is presented in Fig. 5. There, we considered the range of $(Y_p)_{PN}$ presented in Table III together with the abundances due to the r process given in [53], shifted $10^{(7.5)}$ upwards for graphical purposes. We applied this shift since we consider it relevant to the pattern of the resulting nucleosynthesis. We see that for $(Y_p)_{PN} \leq 0.22$ lanthanides are produced, but for $(Y_p)_{PN} = 0.24$ their abundances are two

TABLE IV. The same as in Table III, but starting from pure Λ matter. We assume the initial condition $\rho_b = \rho_\Lambda = 2\rho_0$ (therefore, $\rho_n = \rho_p = 0$).

s	T	$(Y_p)_{PN}$
1.0	11.2	0.406
2.0	26.0	0.493
3.0	47.1	0.525
4.0	74.3	0.544

orders of magnitude lower. For $(Y_p)_{PN} \geq 0.26$ no lanthanides are produced at all.

If we analyze these results together with the values of $(Y_p)_{PN}$ presented in Table III, we have to conclude that, depending on the initial baryon number density (and then the particle composition) of the material that undergoes decompression, a detailed treatment of the Λ hyperon decay is very relevant to find the final nucleosynthesis of the event and, in particular, if it produces lanthanides and heavier isotopes or not. In our opinion, this is the main finding of this paper.

As discussed, in this work we have shown a model for the decay of the Λ component of the ejected matter in a NS-NS merger. We assume an EOS which has Λ matter. It is possible to have a different EOS without Λ 's, but with the same value for $(Y_p)_{PN}$. In this case, the final product would be indistinguishable from ours. If the EOS does have Λ 's, we have developed a model to manage the decay and we have concluded that the Λ 's have a sizable effect on the value of $(Y_p)_{PN}$ and, therefore, on the final nucleosynthesis. Due to the uncertainty in the knowledge of the EOS, this result does not imply a way to demonstrate the presence of Λ matter in a NS-NS merger. However, a theoretical possibility is matter entirely made up of Λ 's, which is discussed in the next subsection. In this case, there is no way out but to implement some model for the Λ decay.

C. The case of strange stars

Let us consider the extreme possibility of the collision of stars made up of strange quark matter up to their surface (SQS). Here we shall consider that this material behaves as a gas of close-packed Λ 's, as proposed long ago by Bethe, Brown, and Cooperstein [17]. Usually, in the literature it has been considered that the surface density of these hypothetical stars is around two times that of nuclear saturation density (see, e.g., [16]). It is a current issue and a recent work [54] explored the possibility that the event GW 190814 was a BH-SQS system, where the SQS can have a mass $M \approx (2.5-2.67)M_\odot$. So, we shall assume it and compute the decay of hyperons in protons and neutrons with the same techniques described above. The results of these calculations are shown in Table IV.

We notice that the values of $(Y_p)_{PN}$ are markedly higher than those found starting from a NS composition. This has a direct consequence for the final nucleosynthesis products. We performed the corresponding calculations as described in Sec. III B assuming that matter undergoes its expansion with the same characteristics as there, but with the values of $(Y_p)_{PN}$

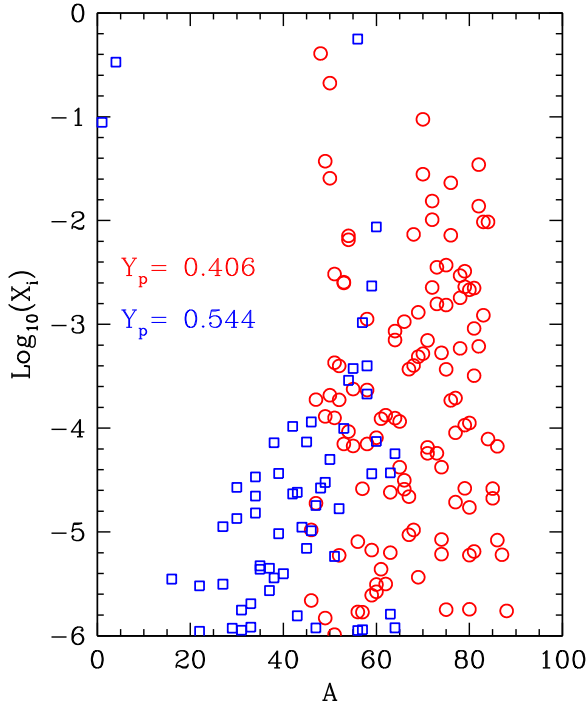


FIG. 6. Abundances per mass unit for the most abundant isotopes resulting from the expansion of matter resulting from the collision of strange stars. Notice that the isotopes are far lighter than those found for the case of the expansion of NS matter with hyperons. In particular, lanthanides are not synthesized at all. Abundances are given in mass fractions.

given in Table IV. The results are shown in Fig. 6. As can be expected, the resulting isotopes are far lighter than those found for the case of NS matter expansion. In particular, we find that lanthanides are not synthesized at all. Evidently, this provides a way for distinguishing strange stars from NSs: the final nucleosynthesis resulting from the collision of each type of star is completely different.

IV. DISCUSSION AND CONCLUSIONS

In this paper we have studied the expansion of neutron star (NS) matter containing a non-negligible fraction of Λ particles from densities above nuclear saturation density up to the end of nucleosynthesis. This process may occur in nature in the collision of two NSs or a NS with a black hole. The Λ hyperons decay by means of mesonic reactions (1) and (2) or, if proton and neutron densities are non negligible, nonmesonic reactions (3) and (4). Hyperons Λ exhaust on a timescale so short that their decay is decoupled from the hydrodynamic expansion of matter. When proton and neutron matter is diluted enough, the formation of helium and heavier nuclei releases an amount of energy large enough to increase its temperature to values high enough to result in conditions of nuclear statistical equilibrium with high entropy per baryon [51]. From then on, nucleosynthesis proceeds and the final composition is largely determined by the proton per baryon fraction Y_p .

It is worth mentioning that the Λ decays described in this work show a very different behavior than the same decays in hypernuclei: for hypernuclei with $A \gtrsim 12$, the Pauli blocking strongly inhibits the mesonic decay. In our case, the mesonic decay is always important. This is because the finite temperature weakens the Pauli blocking. Another important difference with the hypernuclei case is that we do not have a set of hypernuclei all at the same quantum state, but a chain of decays where each decay modifies the conditions of the next one.

In this paper we have considered a NS matter equation of state [36] that contains Λ hyperons and allows for the existence of objects with a mass $M \gtrsim 2M_\odot$, which is not in conflict with recent detection of massive NSs (see Sec. I). We have assumed the equilibrium composition of matter at some densities given in Table II above the threshold for the occurrence of Λ hyperons and computed its decay. The values of Y_p when hyperons exhaust are presented in Table III. Evidently, hyperon decay affects appreciably the value of Y_p . We computed the subsequent evolution of this material starting out from NSE conditions for the range of Y_p values on an expansion with constant value for the entropy per baryon and an exponentially decaying density. We find that, depending on the initial density of the ejected material, the increase in Y_p due to hyperon decay is sufficient to seriously affect the final isotopic composition of ejected matter. For example, if we consider the case labeled as C in Table II, the value of the proton abundance per baryon increases from $(Y_p)_{NS} = 0.1817$ to the range of $(Y_p)_{NP} = 0.2209-0.2640$ depending on the entropy per baryon, s , considered during the Λ hyperon decay. Changes of proton abundance per baryon of such size are large enough to completely change the final composition of ejected matter from abundant to completely devoid of lanthanides, as shown in Fig. 5.

Although our treatment of nucleosynthesis is very simplified, and does not include the complexity of actual kilonovae events, these results indicate that the presence of Λ hyperons affects the final composition of matter ejected in kilonova events in a sizable way. Unfortunately, our knowledge of the EOS for the problem under consideration is not accurate enough to establish unequivocally the initial composition of the ejected matter. In this work we have shown how to deal with the Λ component of matter under the hypothesis of its existence at the initial time.

We have also considered the collision between the hypothetical so-called strange quark stars, assuming that the decay starts from pure Λ matter, roughly at two times the nuclear saturation density. The decay of this matter leads to values Y_p (given in Table IV) far higher than for the case of NS collisions. This leads to a final composition completely different from the one found by starting with NS matter, with the most abundant isotopes belonging to the neighborhood of iron (see Fig. 6), without lanthanide production. This may provide a new way to differentiate NSs from strange stars.

ACKNOWLEDGMENTS

We are indebted to Isaac Vidaña for the fruitful discussions and for providing us with the partial populations from the

Brueckner-Hartree-Fock EOS. The authors want to acknowledge Jorge E. Horvath for discussions during the initial stages of this research and to F. X. Timmes for making the TORCH code freely available. OGB wants to thank Hector Viturro for his help for employing the TORCH code. This work was partially supported by CONICET, Argentina, under Contract No. PIP00273.

APPENDIX: EXPLICIT EXPRESSIONS FOR THE Λ DECAY WIDTHS

In this Appendix we present explicit expressions for the Λ decay widths. At zero temperature, Γ_{π^0} and Γ_{π^-} are found in [38], while we refer the reader to [39] for the expressions for Γ_n and Γ_p . In the present work we evaluate the Λ decay widths at finite temperature. The corresponding decay widths are easily obtained from the ones at $T = 0$, considering each particle involved and by making the replacement

$$\theta(p_F - |p|) \rightarrow f(E_i, \mu_i, T), \quad (\text{A1})$$

where p is the momentum of the particle and p_F is the Fermi momentum. The particle occupation function $f(E_i, \mu_i, T)$ is given by the Fermi-Dirac one,

$$f(E_i, \mu_i, T) = \frac{1}{1 + \exp\{[E_i(p) - \mu_i(T)]/T\}}, \quad (\text{A2})$$

where $E_i(p)$ is the single-particle energy and μ_i the chemical potential for a particle i . In fact, in this work we consider no strong interaction among the hadrons involved. From this and keeping in mind that we performed a nonrelativistic calculation, for the single-particle energy we have $E_i(p) = m_i + p^2/(2m_i)$. We give the density ρ_i for each particle and from this density we obtain the chemical potential by solving the equation for μ_i ,

$$\rho_i = \int \frac{dp}{(2\pi)^3} f(E_i(p), \mu_i, T), \quad (\text{A3})$$

We show now the expressions for the decay widths.

1. The partial mesonic decay widths

The Feynman diagrams representing the mesonic transition amplitudes are shown in Fig. 1. The mesonic decay widths result from squaring these amplitudes and using the standard rules for the evaluation of diagrams. The result is given and discussed in [38]. Here we reproduce this result, but for finite temperature and differentiating the two isospin channels. As a first step, it is convenient to show the partial decay width as a function of the momentum of the Λ particle:

$$\begin{aligned} \tilde{\Gamma}_{\pi^0}(k) &= (G_F m_\pi^2)^2 \int \frac{dq}{(2\pi)^3} \left[A_\pi^2 + \left(\frac{B_\pi}{2m_N} \right)^2 q^2 \right] \\ &\times \theta(k_0 - E_n(k-q)) [1 - f(E_n(k-q), \mu_n, T)] \\ &\times \frac{\pi}{\omega_\pi(q)} \delta(k_0 - E_n(k-q) - \omega_\pi(q)) \end{aligned} \quad (\text{A4})$$

and

$$\begin{aligned} \tilde{\Gamma}_{\pi^-}(k) &= 2 (G_F m_\pi^2)^2 \int \frac{dq}{(2\pi)^3} \left[A_\pi^2 + \left(\frac{B_\pi}{2m_N} \right)^2 q^2 \right] \\ &\times \theta(k_0 - E_p(k-q)) [1 - f(E_n(k-q), \mu_p, T)] \\ &\times \frac{\pi}{\omega_\pi(q)} \delta(k_0 - E_p(k-q) - \omega_\pi(q)), \end{aligned} \quad (\text{A5})$$

where $k \equiv (k_0, \mathbf{k})$ is the energy-momentum of the Λ particle and (q_0, \mathbf{q}) is the energy-momentum carried by the weak interaction. Here G_F is the Fermi weak coupling constant [$G_F/(\hbar c)^3 = 1.16637(1) \times 10^{-5} \text{ GeV}^{-2}$], and $A_\pi = 1.05$ and $B_\pi = -7.15$ are the parity violating and parity conserving couplings constants. The function $\omega_\pi(q) = \sqrt{q^2 + m_\pi^2}$ is the pion energy. Note that these partial decay widths depends also on the temperature and on the chemical potential of each particle.

2. The partial nonmesonic decay widths

Let us recall that the corresponding transitions amplitudes are depicted in Fig. 2. To give the expressions for Γ_n and Γ_p , it is convenient to define first the partial decay widths,

$$\begin{aligned} \tilde{\Gamma}_{nn}(k) &= (G_F m_\pi^2)^2 \frac{1}{(2\pi)^5} \int dq \int dh S_{nn}(q) f(E_n(h), \mu_n, T) \\ &\times [1 - f(E_n(k-q), \mu_n, T)] \\ &\times [1 - f(E_n(h+q), \mu_n, T)] \\ &\times \theta(q_0) \delta(q_0 - [E_n(h+q) - E_n(h)]), \end{aligned} \quad (\text{A6})$$

$$\begin{aligned} \tilde{\Gamma}_{np}(k) &= (G_F m_\pi^2)^2 \frac{1}{(2\pi)^5} \int dq \int dh S_{np}(q) f(E_p(h), \mu_p, T) \\ &\times [1 - f(E_n(k-q), \mu_n, T)] \\ &\times [1 - f(E_p(h+q), \mu_p, T)] \\ &\times \theta(q_0) \delta(q_0 - [E_p(h+q) - E_p(h)]), \end{aligned} \quad (\text{A7})$$

and

$$\begin{aligned} \tilde{\Gamma}_{pn}(k) &= (G_F m_\pi^2)^2 \frac{1}{(2\pi)^5} \int dq \int dh S_{pn}(q) f(E_p(h), \mu_p, T) \\ &\times [1 - f(E_p(k-q), \mu_p, T)] \\ &\times [1 - f(E_n(h+q), \mu_n, T)] \\ &\times \theta(q_0) \delta(q_0 - [E_n(h+q) - E_p(h)]). \end{aligned} \quad (\text{A8})$$

By assigning momentum values to the different lines in Fig. 2 and by taking into account the momentum conservation, one obtains the different momenta in this equation. For simplicity, in these expressions we have shown only their k dependence, but these partial decay widths depend also on the temperature and the chemical potential of each particle.

The function $S_{NN'}(q)$ contains the information on the weak transition potential and the isospin summation. First we show the partial isospin contribution, given by

$$\begin{aligned} S_{\tau\tau'}(q) &= 4 \{ S_\tau(q) S_{\tau'}(q) + S'_\tau(q) S'_{\tau'}(q) + P_{L,\tau}(q) P_{L,\tau'}(q) \\ &+ P_{C,\tau}(q) P_{C,\tau'}(q) + 2 P_{T,\tau}(q) P_{T,\tau'}(q) \\ &+ 2 S_{V,\tau}(q) S_{V,\tau'}(q) \}, \end{aligned} \quad (\text{A9})$$

where $\tau = 0$ or 1 for the isoscalar and isovector terms of the weak interaction, respectively. The functions $S_\tau(q)$, $S'_\tau(q)$, $P_{L,\tau}(q)$, $P_{T,\tau}(q)$, and $S_{V,\tau}(q)$ are defined in the Appendix B in [39]. The isospin summation for each contribution is

$$\begin{aligned} S_{nn}(q) &= \mathcal{S}_{11}(q) + \mathcal{S}_{00}(q) + \mathcal{S}_{01}(q) + \mathcal{S}_{10}(q), \\ S_{np}(q) &= \mathcal{S}_{11}(q) + \mathcal{S}_{00}(q) - \mathcal{S}_{01}(q) - \mathcal{S}_{10}(q), \\ S_{pn}(q) &= 4\mathcal{S}_{11}(q). \end{aligned} \quad (\text{A10})$$

In what follows, we show how to obtain the final values for the decay widths, from these k -dependent expressions.

3. The mesonic and nonmesonic decay widths

To obtain the values for Γ_{π^0} , Γ_{π^-} , Γ_n , and Γ_p , we average the corresponding partial decay widths as

follows:

$$\Gamma_\alpha = \frac{1}{\rho_\Lambda} \int \frac{dk}{(2\pi)^3} f(k_0, \mu_\Lambda, T) \tilde{\Gamma}_\alpha(k), \quad (\text{A11})$$

where $k_0 = E_\Lambda(k) = m_\Lambda + k^2/(2m_\Lambda)$. It is straightforward to see that $\alpha = \pi^0, \pi^-, n$, and p . Note that $\tilde{\Gamma}_n(k) = \tilde{\Gamma}_{nn}(k)$ and $\tilde{\Gamma}_p(k) = \tilde{\Gamma}_{np}(k) + \tilde{\Gamma}_{pn}(k)$.

Before we end this Appendix, it is convenient to discuss the functional dependence of the decay widths Γ_α . It is clear that it depends on the temperature and, from Eq. (A11), also on μ_Λ (the Λ chemical potential). From Eq. (A3) we can see that a dependence on a chemical potential is equivalent to a dependence on the corresponding density. Summarizing, we can write that the functional dependences of each decay width are the following: $\Gamma_{\pi^0} = \Gamma_{\pi^0}(\rho_n, \rho_\Lambda, T)$, $\Gamma_{\pi^-} = \Gamma_{\pi^-}(\rho_p, \rho_\Lambda, T)$, $\Gamma_n = \Gamma_n(\rho_n, \rho_\Lambda, T)$, and $\Gamma_p = \Gamma_p(\rho_n, \rho_p, \rho_\Lambda, T)$.

-
- [1] B. P. Abbott, R. Abbott, T. D. Abbott, M. R. Abernathy, F. Acernese, K. Ackley, C. Adams, T. Adams, P. Addesso, R. X. Adhikari *et al.*, *Phys. Rev. Lett.* **116**, 241103 (2016).
- [2] B. P. Abbott, R. Abbott, T. D. Abbott, F. Acernese, K. Ackley, C. Adams, T. Adams, P. Addesso, R. X. Adhikari, V. B. Adya *et al.*, *Astrophys. J.* **848**, L12 (2017).
- [3] J. Chadwick, *Nature (London)* **129**, 312 (1932).
- [4] W. Baade and F. Zwicky, *Phys. Rev.* **46**, 76 (1934).
- [5] A. Hewish and S. E. Okoye, *Nature (London)* **207**, 59 (1965).
- [6] A. K. Harding, *Front. Phys.* **8**, 679 (2013).
- [7] S. L. Shapiro and S. A. Teukolsky, *Black Holes, White Dwarfs, and Neutron Stars: The Physics of Compact Objects* (Wiley, New York, 1983).
- [8] J. M. Lattimer and M. Prakash, *Astrophys. J.* **550**, 426 (2001).
- [9] J. M. Lattimer and M. Prakash, *Science* **304**, 536 (2004).
- [10] F. Özel and P. Freire, *Annu. Rev. Astron. Astrophys.* **54**, 401 (2016).
- [11] V. A. Ambartsumyan and G. S. Saakyan, *Sov. Astron.* **4**, 187 (1960).
- [12] N. K. Glendenning, *Astrophys. J.* **293**, 470 (1985).
- [13] N. K. Glendenning and S. A. Moszkowski, *Phys. Rev. Lett.* **67**, 2414 (1991).
- [14] A. R. Bodmer, *Phys. Rev. D* **4**, 1601 (1971).
- [15] E. Witten, *Phys. Rev. D* **30**, 272 (1984).
- [16] C. Alcock, E. Farhi, and A. Olinto, *Astrophys. J.* **310**, 261 (1986).
- [17] H. A. Bethe, G. E. Brown, and J. Cooperstein, *Nucl. Phys. A* **462**, 791 (1987).
- [18] M. A. Alpar, *Phys. Rev. Lett.* **58**, 2152 (1987).
- [19] M. Alford, M. Braby, M. Paris, and S. Reddy, *Astrophys. J.* **629**, 969 (2005).
- [20] P. B. Demorest, T. Pennucci, S. M. Ransom, M. S. E. Roberts, and J. W. T. Hessels, *Nature (London)* **467**, 1081 (2010).
- [21] J. Antoniadis, P. C. C. Freire, N. Wex, T. M. Tauris, R. S. Lynch, M. H. van Kerkwijk, M. Kramer, C. Bassa, V. S. Dhillon, T. Driebe *et al.*, *Science* **340**, 1233232 (2013).
- [22] H. T. Cromartie, E. Fonseca, S. M. Ransom, P. B. Demorest, Z. Arzoumanian, H. Blumer, P. R. Brook, M. E. DeCesar, T. Dolch, J. A. Ellis *et al.*, *Nat. Astron.* **4**, 72 (2020).
- [23] Y. Sekiguchi, K. Kiuchi, K. Kyutoku, and M. Shibata, *Phys. Rev. Lett.* **107**, 211101 (2011).
- [24] A. Bauswein, N.-U. F. Bastian, D. B. Blaschke, K. Chatziioannou, J. A. Clark, T. Fischer, and M. Oertel, *Phys. Rev. Lett.* **122**, 061102 (2019).
- [25] E. R. Most, L. J. Papenfort, V. Dexheimer, M. Hanauske, S. Schramm, H. Stöcker, and L. Rezzolla, *Phys. Rev. Lett.* **122**, 061101 (2019).
- [26] P. A. Seeger, W. A. Fowler, and D. D. Clayton, *Astrophys. J. Suppl.* **11**, 121 (1965).
- [27] D. D. Clayton, *Principles of Stellar Evolution and Nucleosynthesis* (Wiley, New York, 1968).
- [28] F. Kappeler, H. Beer, and K. Wisshak, *Rep. Prog. Phys.* **52**, 945 (1989).
- [29] A. Burrows, J. Hayes, and B. A. Fryxell, *Astrophys. J.* **450**, 830 (1995).
- [30] J. M. Lattimer and D. N. Schramm, *Astrophys. J.* **192**, L145 (1974).
- [31] J. J. Cowan, C. Sneden, J. E. Lawler, A. Aprahamian, M. Wiescher, K. Langanke, G. Martínez-Pinedo, and F.-K. Thielemann, *Rev. Mod. Phys.* **93**, 015002 (2021).
- [32] N. R. Tanvir, A. J. Levan, A. S. Fruchter, J. Hjorth, R. A. Hounsell, K. Wiersema, and R. L. Tunnicliffe, *Nature (London)* **500**, 547 (2013).
- [33] D. Kasen, B. Metzger, J. Barnes, E. Quataert, and E. Ramirez-Ruiz, *Nature (London)* **551**, 80 (2017).
- [34] E. Pian, P. D'Avanzo, S. Benetti, M. Branchesi, E. Brocato, S. Campana, E. Cappellaro, S. Covino, V. D'Elia, J. P. U. Fynbo *et al.*, *Nature (London)* **551**, 67 (2017).
- [35] D. Watson, C. J. Hansen, J. Selsing, A. Koch, D. B. Malesani, A. C. Andersen, J. P. U. Fynbo, A. Arcones, A. Bauswein, S. Covino *et al.*, *Nature (London)* **574**, 497 (2019).
- [36] D. Logoteta, I. Vidaña, and I. Bombaci, *Eur. Phys. J. A* **55**, 207 (2019).
- [37] M. Tanabashi, K. Hagiwara, K. Hikasa, K. Nakamura, Y. Sumino, F. Takahashi, J. Tanaka, K. Agashe, G. Aielli, C. Amsler *et al.*, *Phys. Rev. D* **98**, 030001 (2018).
- [38] P. F. De Cordoba and E. Oset, *Nucl. Phys. A* **528**, 736 (1991).
- [39] E. Bauer, *Nucl. Phys. A* **796**, 11 (2007).

- [40] E. Bauer, G. Garbarino, and C. A. Rodríguez Peña, *Phys. Rev. C* **92**, 014301 (2015).
- [41] E. Bauer and G. Garbarino, *Phys. Lett. B* **698**, 306 (2011).
- [42] E. Bauer and G. Garbarino, *Phys. Lett. B* **716**, 249 (2012).
- [43] M. Kim, S. Ajimura, K. Aoki, A. Banu, H. Bhang, T. Fukuda, O. Hashimoto, J. I. Hwang, S. Kameoka, B. H. Kang *et al.*, *Phys. Rev. Lett.* **103**, 182502 (2009).
- [44] E. Bauer, G. Garbarino, A. Parreño, and A. Ramos, *Nucl. Phys. A* **836**, 199 (2010).
- [45] Available at <http://cococubed.asu.edu>.
- [46] D. Kasen, R. Fernández, and B. D. Metzger, *Mon. Not. R. Astron. Soc.* **450**, 1777 (2015).
- [47] A. Parreño, A. Ramos, and C. Bennhold, *Phys. Rev. C* **56**, 339 (1997).
- [48] V. G. J. Stoks and T. A. Rijken, *Phys. Rev. C* **59**, 3009 (1999).
- [49] T. A. Rijken, V. G. J. Stoks, and Y. Yamamoto, *Phys. Rev. C* **59**, 21 (1999).
- [50] G. F. Burgio, H. J. Schulze, and A. Li, *Phys. Rev. C* **83**, 025804 (2011).
- [51] C. Freiburghaus, S. Rosswog, and F. K. Thielemann, *Astrophys. J.* **525**, L121 (1999).
- [52] R. Fernández and B. D. Metzger, *Mon. Not. R. Astron. Soc.* **435**, 502 (2013).
- [53] C. Sneden, J. J. Cowan, and R. Gallino, *Annu. Rev. Astron. Astrophys.* **46**, 241 (2008).
- [54] I. Bombaci, A. Drago, D. Logoteta, G. Pagliara, and I. Vidana, *Phys. Rev. Lett.* **126**, 162702 (2021).